CHINESE OPTICS LETTERS

Vol. 22, No. 5 | May 2024

# Large aperture disk standing-wave unstable resonator with intra-cavity adaptive correction

Yi Yu (于 益)[1,2,3], Jiayu Yi (易家玉)[3], Liu Xu (徐 浏)[3], Jianli Shang (尚建力)[3], Jing Wu (吴 晶)[3], Lixin Tong (童立新)[3*], Qingsong Gao (高清松)[3], Chun Tang (唐 淳)[3], Wei Zhang (张 卫)[3], and Lei Chen (陈 磊)[1]

[1] Department of Optical Engineering, Nanjing University of Science and Technology, Nanjing 210094, China

[2] Graduate School of China Academy of Engineering Physics, Beijing 100193, China

[3] Institute of Applied Electronics, China Academy of Engineering Physics, Mianyang 621900, China

*Corresponding author: yxwsnail@163.com

Received November 18, 2023 | Accepted January 12, 2024 | Posted Online May 14, 2024

An unstable resonator with seven large aperture ceramic disks and intra-cavity adaptive correction is presented. The composite ceramic disks with absorption rings were adopted to suppress amplified spontaneous emission. An intra-cavity aberration non-conjugate correction based on round-trip wavefront and relaxation iteration was applied in the resonator. After tilt and defocus were corrected in turn, an average output power of 4.5 kW was obtained. The corresponding beam quality factor $\beta$ was 19.5. After tilt, defocus, and high order aberrations were corrected, the average output power was increased to 5.4 kW, and the beam quality factor $\beta$ was improved to 6.8.

**Keywords:** Nd:YAG disk; unstable resonator; intra-cavity adaptive optics; composite ceramic.
**DOI:** 10.3788/COL202422.051401

## 1. Introduction

Since the concept of the thin disk laser (TDL) was proposed by Giense[1], there has been much research on TDLs in continuous-wave (CW) operation and short pulsed operation[2,3]. The gain of TDLs is very low due to the quasi-three-level gain media and a thickness of around 200 μm. To achieve high power laser output with high beam quality, a large mode stable resonator or low magnification unstable resonator has to be applied, which are extremely sensitive to misalignment and aberration. Even if ten Yb:YAG disks were applied in the resonator, the magnification parameter was only improved to 1.4[4].

The use of Nd-doped materials in large aperture disk geometry has attracted attention for high effective emission cross-section and negligible re-absorption effect. Ongstad *et al.* developed an 8 cm diameter Nd:YAG spinning disk with 323 W absorbed pump power, generating a CW output power of 200 W[5]. In 2009, Tang *et al.* presented a 3 kW unstable resonator with 7 large aperture Nd:YAG disks[6]. In 2021, Ding *et al.* used a Nd:LuAG ceramic disk stable resonator to obtain output energy of 4.5 J at 10 Hz repetition[7].

Large aperture disk laser resonators suffer from the amplified spontaneous emission (ASE) and aberrations. The usual way to suppress ASE is to roughen the sides of the large aperture disks. Another promising way to overcome this problem is to utilize the composite disk with an undoped layer, which acts as an anti-ASE cap and was proposed to reduce the effective ASE path[8]. Aberrations in unstable resonators have a noticeable impact on the laser mode and output power[9]. Aberration correction in high power unstable resonators with large aberrations is essential. Compared to extra-cavity correction, intra-cavity aberration correction provides additional benefits such as control laser mode and output power. In an unstable ring resonator or an unstable image resonator, the surface shape of the deformation mirror conjugates with the aberration of the gain medium[4,10]. The conventional adaptive optics system can be conveniently adopted without a complex control algorithm to generate stable output. In a standing wave unstable resonator with intra-cavity adaptive corrections, there is no one-to-one analytical correspondence between the measured wavefront and the wavefront that needs to be used as compensation. Sophisticated algorithms are demanded to control the adaptive optics system. In 2004, high-order, adaptive control of the unstable resonator in the solid-state, heat-capacity laser using a deformable mirror (DM) was achieved, as reported by LaFortune *et al.*[11], in which the relationship between the output phase of the laser and the correction was approximated by a linear theory. And far-field images of selected pulses showed a notable performance of correction during a 40-pulse run. However, aberrations and corresponding longitudinal positions are demanded for the correction algorithms. It is impossible to measure the aberration of every disk in different positions in a multiple disk laser with a traditional standing wave unstable resonator.

In this paper, a standing-wave unstable resonator with seven composite ceramic disks is demonstrated. ASE suppression of absorption ring and intra-cavity aberration correction based on round-trip wavefront (RTWF) and relaxation iteration have been investigated. After the intra-cavity correction, both output power and beam quality are improved significantly.

## 2. Design and Experimental Setup

### 2.1. System and schematic layout

The schematic diagram of the ceramic disk laser system is shown in Fig. 1. A positive-branch unstable cavity with magnification factor $M$ of 2 has been adopted. In the cavity, the M1 was a convex mirror with a radius curvature of −12 m, the M2 was a concave mirror with a radius curvature of 24 m, the output coupler (OC) was a scraper, seven ceramic disks were arranged in a row, and the M3, M4, DM1, and DM2 were used to fold laser beam. All of them except the seven disks were coated for high reflectivity at 633 nm and 1064 nm.

To align the cavity, a 1064 nm guide laser (GL) was directed into the cavity through a pinhole in the center of the M2. To detect aberrations, a 633 nm probe light (PL) was guided into and out of the cavity by two dichroic mirrors M5 ($T > 99.7\%$ at 1064 nm, $R = 50\%$ at 633 nm). The RTWF in the PL was measured by a Hartman wavefront sensor (HWS).

The drift mirror (M4) driven by two motors was set to correct tilt. The DM1 driven by an actuator in the center was set to correct defocus. The DM2 driven by 67 actuators was set for all aberrations. Compensating capabilities of the three correctors are shown in Table 1.

The DM2 had both high spatial frequency and response frequency but only in a ±4 μm stroke. When we compensate the static tilt and defocus in a large stroke with the M4 and DM1, the dynamic range of the DM2 would not be wasted for lower orders.

### 2.2. Disk gain module

A disk gain module structure is shown in Fig. 2. A composite ceramic disk was directly welded to a water-cooled copper heat sink with indium solder. The disk is pumped by five laser diode stacks (LDSs). Each stack comprises 60 laser diode bars, providing a maximum peak pump power of 15 kW at 806 nm. The pulse width was 250 μs, and the repetition frequency was 200 Hz. The diode light was focused into a hexagonal waveguide, and the uniform circle spot at the exit of the waveguide truncated by a diaphragm was imaged by a pair lens to a circle spot with a diameter of 60 mm on the double-pass-pumped disk. The efficiency of the entire coupling system was 88%, and the pump uniformity root mean square (RMS) was 90%.

The disk was a piece of composite ceramic disk with the dimensions of 1.5 mm in thickness and 80 mm in diameter. The disk's upper surface was coated for high transmission at 633 nm, 808 nm, and 1064 nm, and its lower surface was coated for high reflectivity at 633 nm, 808 nm, and 1064 nm. A photograph of the composite ceramic disk is shown in Fig. 3. The disk was composed of a 2% (atomic fraction) doped Nd:YAG core with a diameter of 60 mm and a 5% (atomic fraction) doped Sm:YAG ring with a width of 10 mm. One of absorption bands of $Sm^{3+}$ ions in YAG appears in the near infrared (1050–1100 nm) wavelength region with a maximum at about 1070 nm. The absorption coefficients at 1064 and 808 nm of 5% Sm:YAG ceramic sample are 2.29 and 0.09 $cm^{-1}$. Sm:YAG was found to be the best material for suppressing ASE of Nd:YAG gain medium pumped by an 808 nm LD[12].

**Table 1.** Compensating Capabilities of Correcting.

| Devices | | Correction Range | Control Bandwith |
|---|---|---|---|
| M4 | Tilt | ±10 mrad | 10 Hz |
| DM1 | Defocus | 20 μm | 10 Hz |
| DM2 | PV | 8 μm | 50 Hz |
| | RMS | 1 μm | |

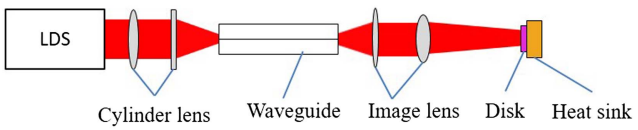


**Fig. 2.** Schematic of the disk gain module.

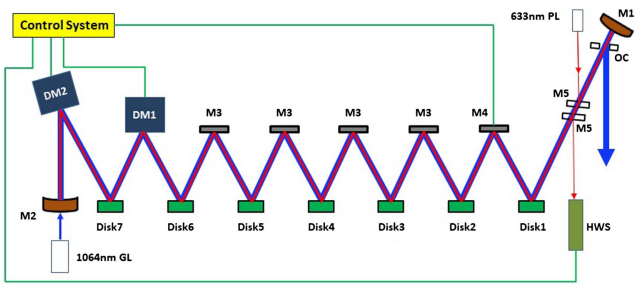


**Fig. 1.** Experimental setup of the disk standing-wave unstable resonator.

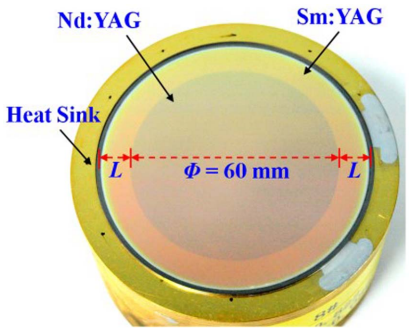


**Fig. 3.** Photo of the composite ceramic disk.

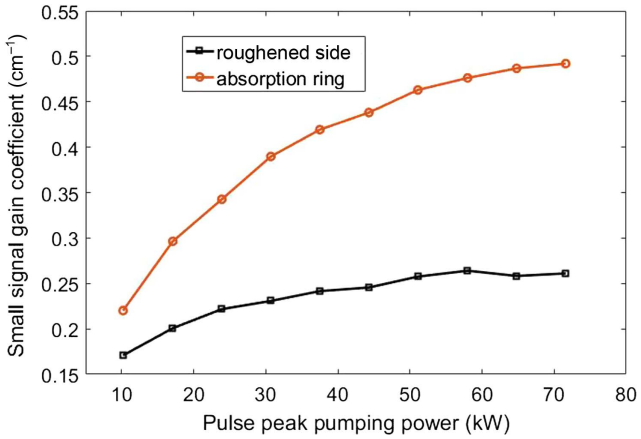


**Fig. 4.** Small signal gain coefficient versus pulse peak pumping power.

In order to evaluate ASE suppression, small signal gain coefficients of both a composite disk with absorption ring and a monolithic disk with a roughened side were measured. The monolithic disk with a roughened side was the same as the core of the composite disk. The small signal gain coefficient as a function of pulse peak pump power is shown in Fig. 4. Obviously, the absorption ring is more effective for suppressing ASE than the roughened side.

### 2.3. Intra-cavity adaptive correction

In a standing-wave unstable non-image cavity with intra-cavity adaptive correction, it is the best correction that a plane wave could retrieve after a round trip. The accurate wavefront for the corrector cannot be obtained directly from the RTWF in PL, but it should be similar to the conjugation of the RTWF. So the product of a factor and the conjugation of the RTWF is assigned to the corrector as a tentative correction. After a number of iterations, an approximate correction would converge to the optimal. If there are multiple correctors for different aberrations in an unstable resonator, the intra-cavity adaptive correction for the $j$th corrector based on RTWF and relax iteration could be described as follows.

The RTWF $\varphi_{\text{out}}^{(1)}(r,\theta)$ in the PL is measured, and the aberration $\varphi_{\text{out},j}^{(1)}(r,\theta)$ is filtered. The additional wavefront $-(\tau/2)\cdot\varphi_{\text{out},j}^{(1)}(r,\theta)$ is set to the corresponding $j$th corrector, where $\tau$ is a relaxation factor, $\tau\in(0,1)$. The RTWF in the PL evolves into $\varphi_{\text{out}}^{(2)}(r,\theta)$. Repeat the above process until the aberration $\varphi_{\text{out},j}^{(n)}(r,\theta)$ converges. The total additional wavefront for the $j$th corrector is

$$\Phi_j(r,\theta)=-(\tau/2)\sum_{i=1}^{n-1}\Phi_{\text{out},j}^{(i)}(r,\theta). \tag{1}$$

To avoid coupling effects caused by the three correctors in the disk laser, the controlling process logic of three correctors is shown in Fig. 5. By expanding the RTWF in Zernike

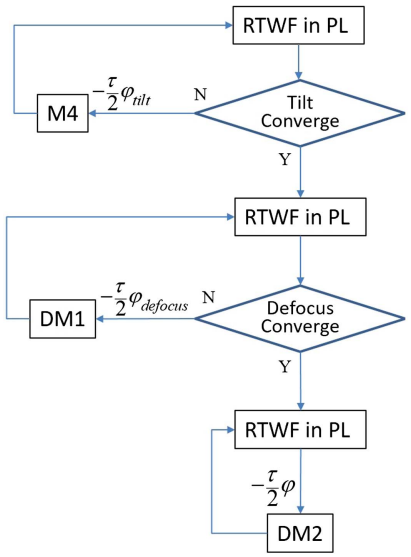


**Fig. 5.** Logical diagram of synergic controlling process.

polynomials, the tilt and the defocus are successively filtered and corrected with the method based on the RTWF and relaxation iteration. When the tilt and the defocus of RTWF converge, the loops are terminated, and the final status of the correctors (M4, DM1) is retained. The static proportion of tilt and defocus is compensated. The residual tilt, defocus, and high order aberrations are corrected by the DM2 with the same method. Owing to the fast-variation aberrations, the closed-loop correction with the DM2 should be maintained all the while.

## 3. Experimental Results and Discussion

By pumping with a pulse peak power of 525 kW, a repetition frequency of 200 Hz, and a pulse width of 250 μs, the average output power extracted from the resonator as a function of the time is shown in Fig. 6, and the RTWF in PL and the far-field spot of the output laser are shown in Fig. 7. Beam quality factor $\beta$ was measured to evaluate the correction result. The beam quality

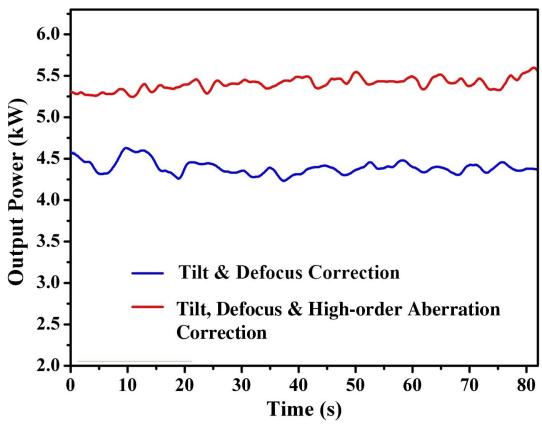


**Fig. 6.** Average output power versus time.

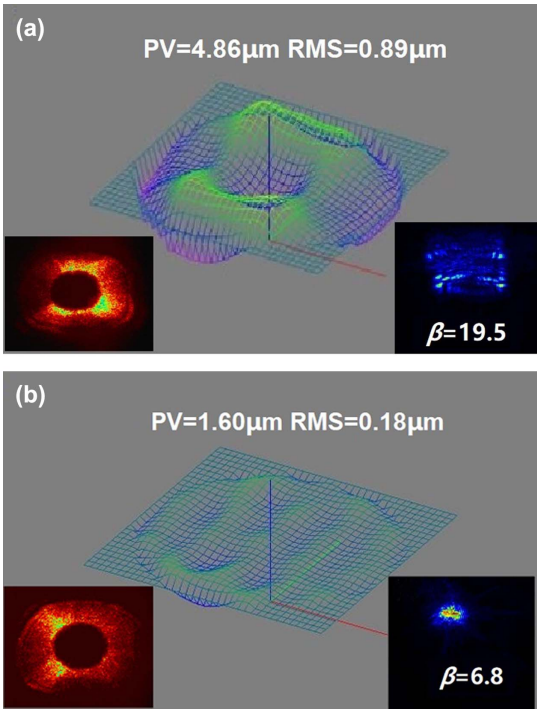


**Fig. 7.** (a) The RTWF after tilt and defocus correction (the corresponding profiles of the near field and far field are shown in the insets). (b) The RTWF after tilt, defocus, and high order aberrations correction (the corresponding profiles of the near field and far field are shown in the insets).

factor $\beta$ was deduced by the ratio between the actual divergence angle measured in experiment and the simulated divergence angle of the ideal annular plane wave with an obscure ratio of 0.5.

Steady output power was not measured without any correction. After tilt and defocus corrections, an output power of 4.5 kW was obtained, and the RMS of the RTWF converged to 0.89 μm, and the beam quality factor $\beta$ was 19.5. When the DM2 began to correct the residual tilt, defocus, and high order aberrations, the RMS of the RTWF converged from 0.89 μm to 0.18 μm after 5 iterations (Fig. 8). The output power was increased to 5.4 kW, and the beam quality factor $\beta$ was improved

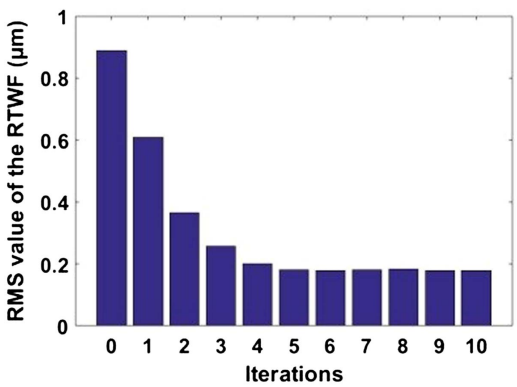


**Fig. 8.** The RMS value of the RTWF versus iterations.

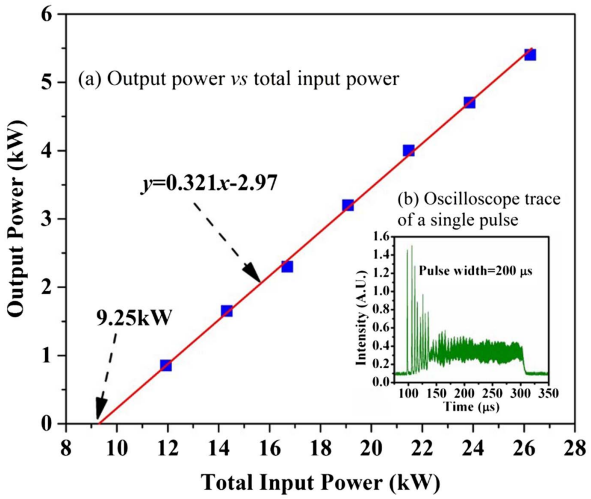


**Fig. 9.** (a) The output power versus total input power. The inset (b) shows the oscilloscope trace of a single pulse.

to 6.8. Both output power and beam quality had remarkable improvement after intra-cavity aberration corrections. Due to considerable correction residuals, the beam quality was not good enough. The main reasons could be inadequate correction capability for high order aberrations and significant decline in closed-loop bandwidth caused by the iterations. It was inferred that better beam quality could be obtained if the DM2 has more actuators and higher control bandwidth.

After tilt, defocus, and high order aberration corrections, the average output power extracted from the resonator as a function of total input power is shown in Fig. 9(a) at a repetition frequency of 200 Hz. A maximum output power of 5.4 kW was achieved with an optical-optical efficiency of 20.6%. The slope efficiency was 32.1%, and the pump threshold was approximately 9.25 kW. Figure 9(b) shows the oscilloscope trace of the disk laser measured at full output power. The pulse width of the laser was about 200 μs, and it is less than the pulse width of the pumping source (250 μs) as a result of buildup time of the laser oscillation.

## 4. Conclusion

A standing-wave unstable resonator with seven large aperture composite ceramic disks and intra-cavity adaptive correction is presented. The absorption ring is found to be more effective to suppress the ASE of large aperture disks than the roughened side.

A universal intra-cavity aberration non-conjugate correction is realized based on RTWF and relaxation iteration. At the maximum pumping power, steady laser output was not acquired without any correction. After tilt and defocus were corrected in turn, an average output power of 4.5 kW was obtained. The corresponding beam quality factor $\beta$ was 19.5. After tilt, defocus, and high order aberrations were corrected, the average output power was increased to 5.4 kW, and the beam quality factor $\beta$ was improved to 6.8.

## Acknowledgements

This work was supported by the National Natural Science Foundation of China (No. 62105313).

## References

1. A. Giesen, H. Hügel, A. Voss, *et al.*, "Scalable concept for diode-pumped high-power solid-state lasers," Appl. Phys. B **58**, 365 (1994).
2. E. Papastathopoulos, F. Baumann, O. Bocksrocker, *et al.*, "High-power high-brightness disk lasers for advanced applications," Proc. SPIE **11664**, 116640M (2021).
3. T. Nubbemeyer, M. Kaumanns, M. Ueffing, *et al.*, "1 kW, 200 mJ picosecond thin-disk laser system," Opt. Lett. **42**, 1381 (2017).
4. M. D. Nixon and M. C. Cates, "High energy high brightness thin disk laser," Proc. SPIE **8547**, 85470D (2012).
5. A. P. Ongstad, M. R. Guy, and J. R. Chavez, "High power Nd:YAG spinning disk laser," Opt. Express **24**, 108 (2016).
6. C. Tang, Z. Yao, J. Jiang, *et al.*, "High-average power disk laser face-pumped by 2D-stack diode arrays," Proc. SPIE **7131**, 713113 (2009).
7. J. Ding, J. Wang, G. Yu, *et al.*, "Theoretical and experimental study of diode-pumped Nd:LuAG disk lasers," Proc. SPIE **11849**, 1184910 (2021).
8. A. Aleknavičius, M. Gabalis, A. Michailovas, *et al.*, "Aberrations induced by anti-ASE cap on thin-disk active element," Opt. Express **21**, 14530 (2013).
9. X. Zhang, J. Wang, and Z. Hu, "Wavefront aberration analysis in misalignment passive positive-branch unstable laser resonators," Optik **127**, 3912 (2016).
10. C. Yang, B. Xu, B. Lai, *et al.*, "Intra-cavity adaptive correction of a unidirectional Nd:YAG slab unstable travelling-wave resonator," IEEE Photon. Technol. Lett. **33**, 1333 (2021).
11. K. N. LaFortune, R. L. Hurd, E. M. Johansson, *et al.*, "Intracavity adaptive correction of a 10 kW, solid-state, heat-capacity laser," Proc. SPIE **5333**, 53 (2004).
12. A. D. Timoshenko, O. O. Matvienko, A. G. Doroshenko, *et al.*, "Highly-doped YAG:$Sm^{3+}$ transparent ceramics: effect of $Sm^{3+}$ ions concentration," Ceram. Int. **49**, 7524 (2023).